low resolution and high noise common to dynamic SPECT, as well as the fact that the projections are acquired sequentially, make it questionable as to whether a similar method could work for dynamic cardiac SPECT studies. We chose to implement the oblique rotation step in FADS by minimizing the difference between the original data and their representation in the space spanned by the principal components, while the factor coefficients and the time-activity curves were constrained to be non-negative.

The method was validated in 2-D with a realistic simulation of the dynamic SPECT imaging process, using the anatomically correct MCAT phantom. Poisson noise was incorporated into the projections at a count level derived from dog experiments. Testing was also performed on dynamic Tc-99m teboroxime canine data. In both cases, transaxials were reoriented to short axis slices. The image was cropped to a central 11x11 pixels (8cmx8cm). The FADS method extracted from the simulation an input function that appeared closer to the true blood time-activity curve than did the curve from a manually chosen ROI. Curves extracted with FADS from the canine data appeared similar to curves from manual ROIs, but generally had a lower tail. This is likely due to less tissue contamination with the FADS method.

The FADS method did not work in every case tested. However, we have shown that the high noise and poor resolution intrinsic to dynamic SPECT does not completely thwart the FADS methodology. With further modifications based on *a priori* information and the use of 3-D regions, the FADS approach will likely provide a robust and automatic means to extract the blood and perhaps the tissue components in dynamic SPECT.

No. 24

STRUCTURED BIAS ORIGINATING FROM INTERACTION BETWEEN A PENALIZED OBJECTIVE FUNCTION AND THE SYSTEM MATRIX C.Y. Ng, N.H. Clinthorne, J.A. Fessler, A.O. Hero and W.L. Rogers. Dept. Biomedical Engineering, Division of Nuclear Medicine, EECS Dept., The University of Michigan, Ann Arbor, Michigan, USA

When using a penalized weighted least squares (PWLS) algorithm to reconstruct images for a brain imaging system comprised of a ring tomograph augmented with a single vertex view we noticed that there was substantial smearing of activity between planes even though the regularization or penalty term was only two-dimensional.

To isolate the cause of the problem, we examined the inverse of the Fisher Information Matrix (FIM) which is the bound on the covariance of the raw data. For a conventional 2D tomograph, correlation between pixels only occurs on the same plane, but when vertex data is added, a strong negative covariance is observed for pixels in planes above and below the pixel being examined. To study the effect of regularization on bleed through, we examined the bias gradient vectors. Bias gradient reveals how the changes in true pixel values will affect the mean estimate of the pixel of interest. Again, for the tomograph-only case, we only observed coupling of pixels within the same plane, and increasing the amount of regularization increased the size of the domain of pixels which affect the pixel of interest. When the vertex data is added, the bias gradient increases for pixels above and below the pixel of interest with a distribution similar to the bound on covariance.

Since the PWLS algorithm with ideal weights can be shown to attain the uniform lower bound on variance for a given norm of the bias gradient vector, our interpretation of the bleed through phenomenon is that the longitudinal bias results from averaging along lines of negative covariance to minimize variance. This is allowed to occur because the two dimensional penalty term does not inhibit this spatial distribution of bias, not because it explicitly causes the effect. Bleed through can be substantially reduced by tapering the strength of the penalty term inversely to the vertex collimator resolution at each plane. It may be possible to design a 3-D penalty function that will discourage bleed through at a cost of increasing variance.

This study yields insight into the interrelationship between the system matrix and the objective function that can cause artifacts and suggests approaches to solve the problem.

Oncology Diagnosis: Antibody

12:30-2:00 **Session 5** **Room: Lila Cockrell Theatre**

Moderator: Jorge A. Carrasquillo, MD
Co-moderator: Dave Colcher, PhD

No. 25

RESULTS OF CEA-SCAN® IMMUNOSCINTIGRAPHY IN 59 PATIENTS WITH NON-PALPABLE, MAMMOGRAPHICALLY ABNORMAL BREAST LESIONS. H. A. Nabi, D. Rosner, V. Panaro, D. A. Erb, D. M. Goldenberg; Departments of Nuclear Medicine, Gynecology & Obstetrics and Radiology, State University of New York at Buffalo, Buffalo, NY, and Garden State Cancer Center, Belleville, NJ.

Successful targeting of breast carcinomas with the technetium-99m anti-carcinoembryonic monoclonal antibody Fab' fragment, CEA-Scan® (Immunomedics, Morris Plains, NJ) has been demonstrated recently. In a preliminary study (JNM 1996; 5:238), we have demonstrated a difference in intensity uptake between truly benign, pre-malignant, and malignant lesions.

The purpose of this study is to expand the application of CEA-Scan® mammoscintigraphy in patients with non-palpable, indeterminate mammograms (MM), and determine if CEA-Scan® can improve upon the the low specificity of MM, with the ultimate goal of reducing unnecessary breast biopsies.

Fifty-nine consecutive patients with non-palpable, abnormal mammograms were studied; each received approximately 28 mCi of ^{99m}Tc CEA-Scan. Prone-dependent and dedicated supine views of the mammary glands were obtained within 4-6 hours.

All abnormal MM findings were histologically confirmed (excisional or stereotactic, fine needle) biopsies. Carcinoma was confirmed in 5/41 pts. (12.2%), and 8/18 pts. (44.4%) with low probability/indeterminate and suspicious/highly suspicious MM, respectively.

CEA-Scan® results, corroborated with histology findings, were:

	Sensitivity	Specificity	PPV	NPV
. Low Probability/ Indeterminate	60%	92%	60%	92%
. Suspicious/highly Suspicious	38%	100%	100%	64%
. TOTAL	46%	96%	75%	86%

In the clinically challenging group of pts. with indeterminate MM, CEA-Scan® was far superior to mammography in identifying cancers (60% vs. 12%). Furthermore, because of the high specificity and negative predictive values (92%) in that group of patients, CEA-Scan® may play a significant role in obviating the need for surgical biopsies, as reported by Rosner et al, (ASCO Proc., 1996; 15:102).

No. 26

ANTI-CEA ANTIBODIES VERSUS OCTREOTIDE FOR THE DETECTION OF METASTATIC MEDULLARY THYROID CANCER: ARE CEA AND SOMATOSTATIN-RECEPTOR EXPRESSION PROGNOSTIC FACTORS ? T.M. Behr, S. Gratz, D.L. Munz, W. Becker. Dept. of Nuclear Medicine of the University of Göttingen, Germany.

In medullary thyroid cancer (MTC), postsurgically elevated calcitonin levels frequently indicate metastatic disease, although all conventional diagnostic procedures fail to localize any responsible lesion (occult disease). Anti-CEA antibodies as well as somatostatin analogs have shown promising results in the staging of MTC. The aim of this study was, therefore, to compare the sensitivity of both methodologies intraindividually, as well as to assess possible correlations between the scintigraphic behavior and the patients' prognosis.

A total of 26 patients with MTC was examined between 1977 and 1996: 10 suffered from known, 14 from occult MTC, 2 patients were free of disease at the time of presentation. 16 patients were investigated with anti-CEA MAbs (receiving a total of 35 injections; clones BW431/26, BW431/31, IMACIS, or F023C5, labeled with ^{99m}Tc, ^{111}In or ^{131}I) and ^{111}In-labeled octreotide. All patients underwent conventional radiological evaluation (ultrasonography, CT, MRI) and/or biopsy within four weeks. Clinical follow-up was obtained.

All patients with known disease had elevated plasma CEA (range 6.8-345 ng/ml), whereas in 9/14 occult cases, levels were ≤ 5 ng/ml. In patients with known disease, the overall lesion-based sensitivity was 86% for the anti-CEA MAbs, whereas octreotide was unable to target any tumor in patients with clinically aggressive disease (overall sensitivity only 47%). With octreotide, significantly higher tumor/non-tumor ratios were seen in clinically stable or slowly progressing forms ($p<0.05$), whereas anti-CEA-Mabs yielded highest uptake ratios in rapidly progressing, aggressive disease. In all patients with occult MTC, anti-CEA MAbs as well as octreotide were able to correctly localize at least one lesion (patient-based sensitivity virtually 100%): typically, cervical lymph nodes were identified in post-surgically occult disease, whereas a characteristic "chimney-shaped" bilateral mediastinal involvement was detected in occult MTC several years after primary surgery.

For the staging of MTC, anti-CEA MAbs and octreotide seem to have a sensitivity which is superior to conventional diagnostic modalities, especially when used in combination. Better detectability with anti-CEA antibodies (higher CEA expression ?), may be associated with more aggressive forms, whereas somatostatin receptor expression at normal plasma CEA levels and weak anti-CEA MAb targeting seems to be associated with a more benign clinical course. This is in accordance to the studies of Busnardo et al. and Mendelsohn et al. (*Cancer* 1984; 53: 278 & 54: 657), who showed higher CEA levels to be associated with a worse prognosis, as well as to the *in-vitro* findings of Reubi et al. (*Lab Invest* 1991; 64: 567), who demonstrated the loss of somatostatin receptors in less differentiated MTC.

Boxes 1, 2 and 4 MUST be completed

1 **Fill in** *only* **ONE** letter in *box below.*
This abstract is intended for:
A Technologist program
B Technologist student submission
C Society program
D Scientific exhibit

C

2 **CHECK** *only* **ONE** *box below.*
I am willing to present this paper:
☐ by posterboard only
☑ either oral or posterboard

3 **Eligibility for Special Awards** (Oral Only)
☐ Cardiovascular Young Investigators
☑ Computer and Instrumentation Young Investigators
☐ Berson-Yalow
☐ Pediatric Imaging
☐ Technologist Cardiology
☐ Technologist Brain Imaging

4 **Write** *only* **ONE** *category's abbreviation in the space below:*

CLINICAL SCIENCE/ APPLICATIONS:
Bone/Joint (B/J)
Cardiovascular-Basic (CVB)
Cardiovascular-Clinical (CVC)
Cardiovascular-PET (CVP)
Endocrine (END)
Gastroenterology (GAS)
Hematology/Infectious Disease (HID)
Neurosciences:
Basic (NSB)
Neurology (NSN)
Psychiatry (NSP)
Oncology Diagnosis
FDG (FDG)
Antibody (ODA)
Other (ODO)
Oncology/Therapy (OT)
Pediatrics (PED)
Pulmonary (PUL)
Renal/Hypertension (REH)

INSTRUMENTATION & DATA ANALYSIS
General (GEN)
PET (PET)
SPECT (SPT)

DOSIMETRY/ RADIOBIOLOGY
(DOS)

RADIOASSAY
(RSY)

RADIOPHARMACEUTICAL CHEMISTRY:
Single Photons:
Technetium (TPC)
Other Nuclides (OPC)
Positrons:
F-18 (FPC)
Other Nuclides (CPC)
Therapy Nuclides (YPC)
Radiopharmacy (RPC)
Proteins/Peptides (PPC)

Write *only* **ONE** *category in this space* S P T

1997 ABSTRACT FORM FOR BOTH SCIENTIFIC PAPERS AND SCIENTIFIC EXHIBITS

The Society of Nuclear Medicine 44th Annual Meeting
San Antonio Convention Center
Sunday, June 1–Thursday, June 5, 1997

Do Not Fold Or Bend This Form/Abstract Will Be Published As Typed

№ 35178

Type Abstract Here: (Be sure to stay within border–12.4 × 14.9 cm) (4 ⅞" × 5 ⅞")

STRUCTURED BIAS ORIGINATING FROM INTERACTION BETWEEN A PENALIZED OBJECTIVE FUNCTION AND THE SYSTEM MATRIX

C.Y. Ng, N.H. Clinthorne, J.A. Fessler, A.O. Hero and W.L. Rogers. Dept. Biomedical Engineering, Division of Nuclear Medicine, EECS Dept., The University of Michigan, Ann Arbor, Michigan, USA

When using a penalized weighted least squares (PWLS) algorithm to reconstruct images for a brain imaging system comprised of a ring tomograph augmented with a single vertex view we noticed that there was substantial smearing of activity between planes even though the regularization or penalty term was only two-dimensional.

To isolate the cause of the problem, we examined the inverse of the Fisher Information Matrix (FIM) which is the bound on the covariance of the raw data. For a conventional 2D tomograph, correlation between pixels only occurs on the same plane, but when vertex data is added, a strong negative covariance is observed for pixels in planes above and below the pixel being examined. To study the effect of regularization on bleed through, we examined the bias gradient vectors. Bias gradient reveals how the changes in true pixel values will affect the mean estimate of the pixel of interest. Again, for the tomograph-only case, we only observed coupling of pixels within the same plane, and increasing the amount of regularization increased the size of the domain of pixels which affect the pixel of interest. When the vertex data is added, the bias gradient increases for pixels above and below the pixel of interest with a distribution similar to the bound on covariance.

Since the PWLS algorithm with ideal weights can be shown to attain the uniform lower bound on variance for a given norm of the bias gradient vector, our interpretation of the bleed through phenomenon is that the longitudinal bias results from averaging along lines of negative covariance to minimize variance. This is allowed to occur because the two dimensional penalty term does not inhibit this spatial distribution of bias, not because it explicitly causes the effect. Bleed through can be substantially reduced by tapering the strength of the penalty term inversely to the vertex collimator resolution at each plane. It may be possible to design a 3-D penalty function that will discourage bleed through at a cost of increasing variance.

This study yields insight into the interrelationship between the system matrix and the objective function that can cause artifacts and suggests approaches to solve the problem.

List the name, address, & telephone number of the individual who should receive all correspondence.

Chor-yi, NG
c/o Dr. W. Leslie Rogers
3480 Kresge III
University of Michigan Medical School
Division of Nuclear Medicine
Ann Arbor, MI 48109-0552
Tel: (313)763-3277

List the name and degree of presenting author:

Chor-yi NG, Ph.D.

Reconstruction, SPECT, 3D

TWO KEY WORDS FOR SUBJECT INDEX (See Meeting Memo for details)

(Electronically transmitted facsimiles will NOT be accepted)

DEADLINES
For Scientific Papers and Exhibits: Abstracts must be received (not postmarked) by Thursday, January 9, 1997.
Please note: Acceptance or non-acceptance letters will be mailed March, 1997.

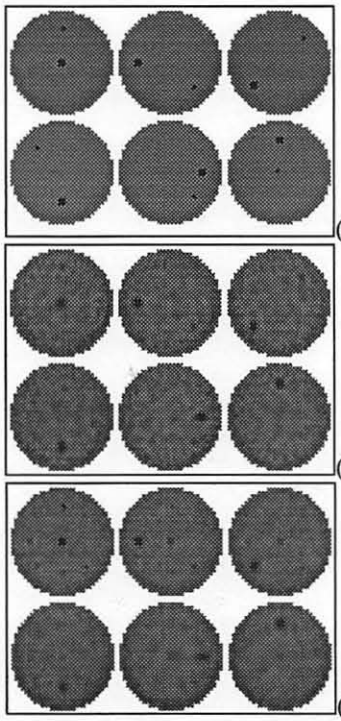

Figure 1(a) Phantom. (b) Reconstructed image with tomograph only data, β=5e-6. (c) Reconstruction image with added vertex data, β=5e-6. Image resolution and noise characteristics are improved but there are bleed through of activities between planes.

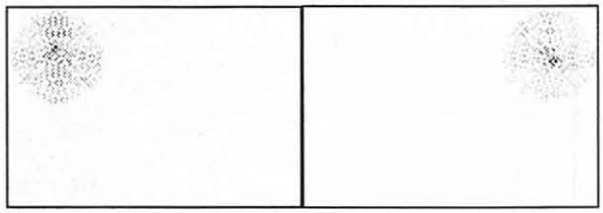

Figure 2: A column of the inverse of FIM arranged as an image for an angularly undersampled tomograph. This can be interpreted as the bound on covariance of the pixel of interest to other pixels. Left: The pixel of interest is a single pixel hot spot on plane 1. Right: Pixel of interest is a single pixel hot spot on plane 3.

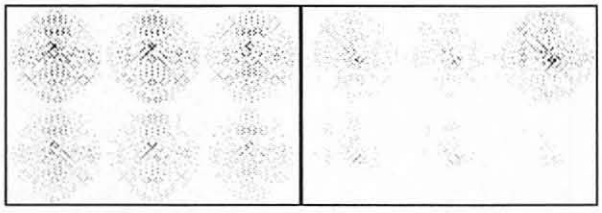

Figure 3: Image of inverse FIM for an angularly undersampled tomograph with vertex detector. Left: Pixel of interest is the single pixel hot spot on plane 1. Right: Pixel of interest is a single pixel hot spot on plane 3.

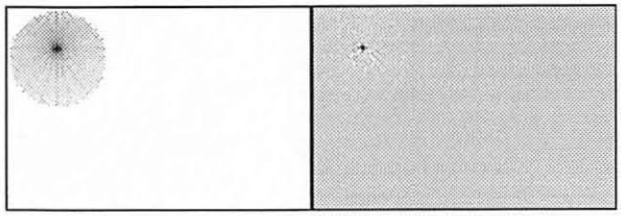

Figure 4: Bias gradient arranged as an image for tomograph for a hot pixel on plane 1. Left: Norm of the bias gradient is 0.9875 which is equivalent to a lot or regularization. Right: Bias gradient norm is 0.2256.

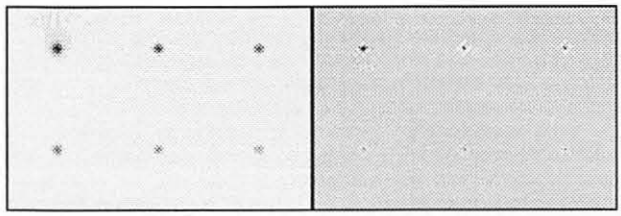

Figure 5: Bias gradient image for tomograph+vertex for a hot pixel on plane 1. Left: Norm of the bias gradient is 0.9940. Right: Bias gradient norm is 0.3320.

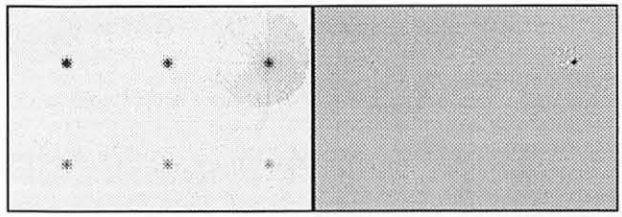

Figure 6: Bias gradient image for tomograph+vertex for a hot pixel on plane 3. Left: Norm of the bias gradient is 0.9940. Right: Bias gradient norm is 0.2779.

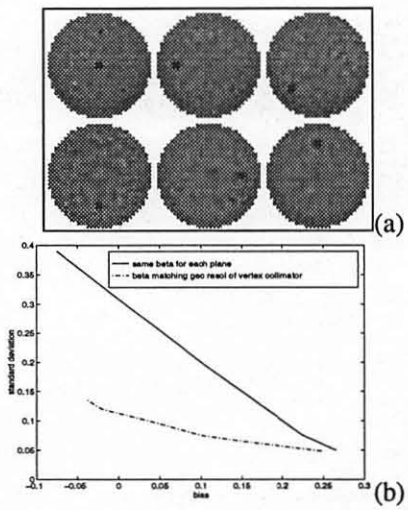

Figure 7(a): Reconstructed image with tapering regularization parameter showing much reduced bleed through. 7(b): Bias and STD comparison of plane 2 center pixel for reconstruction at constant regularization and tapering regularization.